

Equator-S CIS1 Efficiencies

Lynn M Kistler

Jameson Parker

8/12/97

TABLE OF FIGURES:	3
TABLE OF TABLES:	4
INTRODUCTION	5
DETERMINING OPTIMUM MCP EFFICIENCIES.....	5
DETERMINING ION EFFICIENCIES VS. ENERGY	6
INDIVIDUAL ION EFFICIENCIES:	8
O+.....	8
HE+.....	12
HE++.....	16
H+.....	16
N2+.....	21
ESA/ALPHA ACCEPTANCE	26
GEOMETRIC FACTOR	29
GEOMETRIC FACTOR CALCULATION	29
GEOMETRIC FACTOR CONCLUSIONS:.....	30
CONVERSIONS.	32

Table of Figures:

Figure 1: “Stop” Efficiency verse MCP voltage for O+_____	5
Figure 2: “Start” efficiency verses MCP voltage for O+_____	6
Figure 3: “Single Valid Event” efficiency verses MCP voltage for O+_____	6
Figure 4: The total efficiency (product of SFR/PR, SFR/SF and SEV/SFR) verses Total Energy for O+.	7
Figure 5: The total efficiency with pixel adjustment verses Total Energy for HS side O+.	7
Figure 6a: HS side “Start” Efficiency verses Total Energy for O+.	8
Figure 6b: HS side “Stop” Efficiency verses Total Energy for O+.	8
Figure 6c: HS side “Valid Event” Efficiency verses Total Energy for O+.	8
Figure 6d: HS side Total Efficiency verses Total Energy for O+.	9
Figure 6e: HS side Total Efficiency w/ pixel adjustment verses Total Energy for O+.	9
Figure 7a: LS side “Start” Efficiency verses Total Energy for O+.	10
Figure 7b: LS side “Stop” Efficiency verses Total Energy for O+.	10
Figure 7c: LS side “Valid Event” Efficiency verses Total Energy for O+.	10
Figure 7d: LS side Total Efficiency verses Total Energy for O+.	11
Figure 7e: LS side Total Efficiency w/ pixel adjustment verses Total Energy for O+.	11
Figure 8a: HS side “Start” Efficiency verses Total Energy for He+.	12
Figure 8b: HS side “Stop” Efficiency verses Total Energy for He+.	12
Figure 8c: HS side “Valid Event” Efficiency verses Total Energy for He+.	12
Figure 8d: HS side Total Efficiency verses Total Energy for He+.	13
Figure 8e: HS side Total Efficiency w/ pixel adjustment verses Total Energy He+.	13
Figure 9a: LS side “Start” Efficiency verses Total Energy for He+.	14
Figure 9b: LS side “Stop” Efficiency verses Total Energy for He+.	14
Figure 9c: LS side “Valid Event” Efficiency verses Total Energy for He+.	14
Figure 9d: LS side Total Efficiency verses Total Energy for He+.	15
Figure 9e: LS side Total Efficiency w/ pixel adjustment verses Total Energy for He+.	15
Figure 10: He+ and He++, calibration curves shown to 130 keV.	16
Figure 11a: HS side “Start” Efficiency verses Total Energy for H+.	17
Figure 11b: HS side “Stop” Efficiency verses Total Energy for H+.	17
Figure 11c: HS side “Valid Event” Efficiency verses Total Energy for H+.	17
Figure 11d: HS side Total Efficiency verses Total Energy for H+.	18
Figure 11e: HS side Total Efficiency w/ pixel adjustment verses Total Energy H+.	18
Figure 12a: LS side “Start” Efficiency verses Total Energy for H+.	19
Figure 12b: LS side “Stop” Efficiency verses Total Energy for H+.	19
Figure 12c: LS side “Valid Event” Efficiency verses Total Energy for H+.	19
Figure 12e: LS side Total Efficiency w/ pixel adjustment verses Total Energy for H+.	20
Figure 13a: HS side “Start” Efficiency verses Total Energy for N2+.	21
Figure 13b: HS side “Stop” Efficiency verses Total Energy for N2+.	21
Figure 13c: HS side “Valid Event” Efficiency verses Total Energy for N2+.	21
Figure 13d: HS side Total Efficiency verses Total Energy for N2+.	22
Figure 13e: HS side Total Efficiency w/ pixel adjustment verses Total Energy for N2+.	22
Figure 14a: LS side “Start” Efficiency verses Total Energy for N2+.	23
Figure 14b: LS side “Stop” Efficiency verses Total Energy for N2+.	23
Figure 14c: LS side “Valid Event” Efficiency verses Total Energy for N2+.	23
Figure 14d: LS side Total Efficiency verses Total Energy for N2+.	24
Figure 14e: LS side Total Efficiency w/ pixel adjustment verses Total Energy for N2+.	24
Figure 15: ESA/alpha plot for protons with total energy 55 keV.	26
Figure 16: Alpha angles summed for each ESA voltage for the proton with total energy 55 keV.	27
Figure 17: ESA voltages summed for each Alpha angle for the proton with total energy 55 keV.	27
Figure 18: He+, pixel 2 from ‘96 Bern Equator-S calibration. Representative of all files.	31
Figure 19: N2+, pixel 11 from the ‘97 Bern Equator-S calibration.	31

Table of tables:

<i>Table 1: Efficiency curve polynomials and adjustment factors for each ion..</i>	<i>25</i>
<i>Table 2: Equator-S Bern '97 calibration, .</i>	<i>28</i>
<i>Table 3: Geometric factors for the different Cluster models</i>	<i>30</i>
<i>Table 4: Two calibrations sets for the geometric factors on the Equator-S instrument.</i>	<i>30</i>
<i>Table 5: The HS geometric factors of each ion in the Cluster and Equator-S calibrations.</i>	<i>31</i>

Introduction

The total efficiency for measuring an ion in the CODIF (COmposition and DIstribution Function analyzer) is affected by three separate contributions. The efficiency for getting a "Start" signal, the efficiency for getting a "Stop" signal, and the efficiency for getting a "Valid Single Event."

The "Start" efficiency is a function of the number of secondary electrons emitted from the carbon foil, the focusing of the electrons onto the MCP, the MCP active area, and the MCP gain and MCP signal threshold. It is measured using the ratio of the Start-Stop Coincidence rate (SFR) to the "Stop" rate. Because CODIF does not measure the rate of the actual "stop" signal, the Stop Position Signal, PR, is used.

The "Stop" efficiency is a function of the scattering of the ion in the foil (which can scatter it away from the active area), and again of the MCP active area, MCP gain and signal threshold. It is given by the ratio of SFR rate to the "Start" rate, SF.

In order to be a valid event, an ion must also generate not only a start and stop signal, but also a single "start Position" (PF) signal and a "Stop Position" signal (PR). The "Valid Event Efficiency" is given by the ratio of the valid Single event rate, SEV, to SFR. These efficiencies are all a function of energy and species, as well as MCP voltage. Determining the final efficiencies is done in two steps. First the optimum voltage at which to run the MCP's is determined. Then, using the optimum MCP voltage, the efficiencies for each species as a function of energy and position are determined.

Determining Optimum MCP Efficiencies

Figures 1-3 are examples of standard curves of efficiency versus MCP (Micro Channel Plate) voltage. Generally, as the voltage increases, the "Start" and "Stop" efficiencies increase (Figure 1 and 2). However, the "Valid Event" shows a different trend (Figure 3). It reaches a peak and then decreases as the voltage increases. The reason for this is that as the MCP signal gets larger, the crosstalk between adjacent pixels increases, and multiple positions are detected. This invalidates the event. So, determining the optimum MCP voltage is a tradeoff between reaching a level where all MCP's are operating at the plateau of the start and stop efficiencies, and at a level where the crosstalk between the pixels is low. In the examples below, any MCP voltage above 148 or 152 would be acceptable when considering the start and stop efficiencies. However, when examining the valid events efficiency (Figure 3), cross talk is evident for the two highest MCP voltages. Therefore, 148 would be the optimum MCP voltage for the ion in this model. The 148 in decimal setting corresponds to a hex setting of 94.

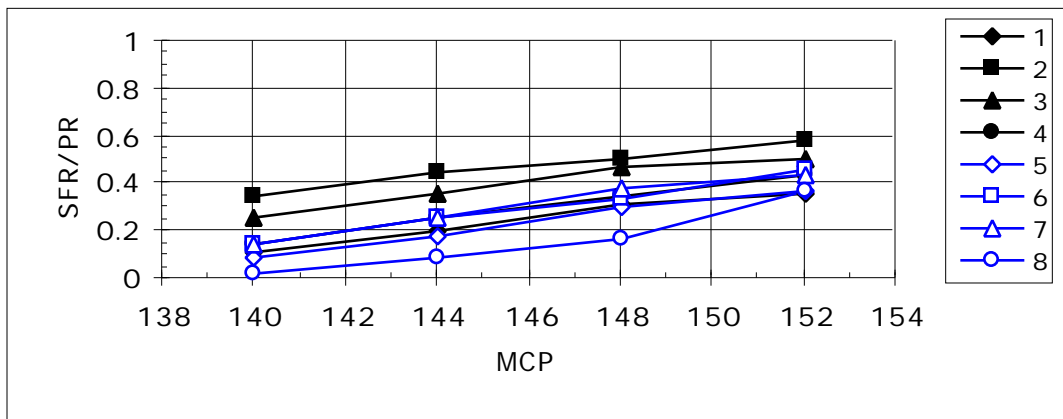


Figure 1: "Stop" Efficiency verse MCP voltage for O+

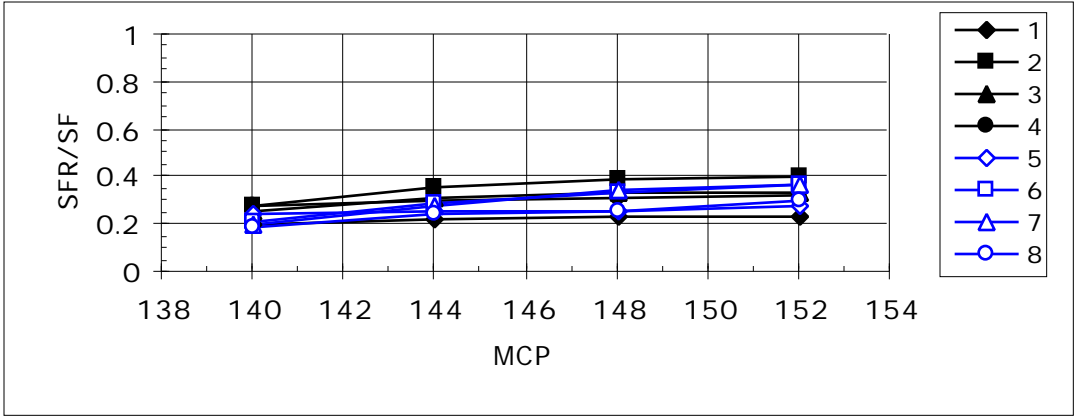


Figure 2: "Start" efficiency versus MCP voltage for O+

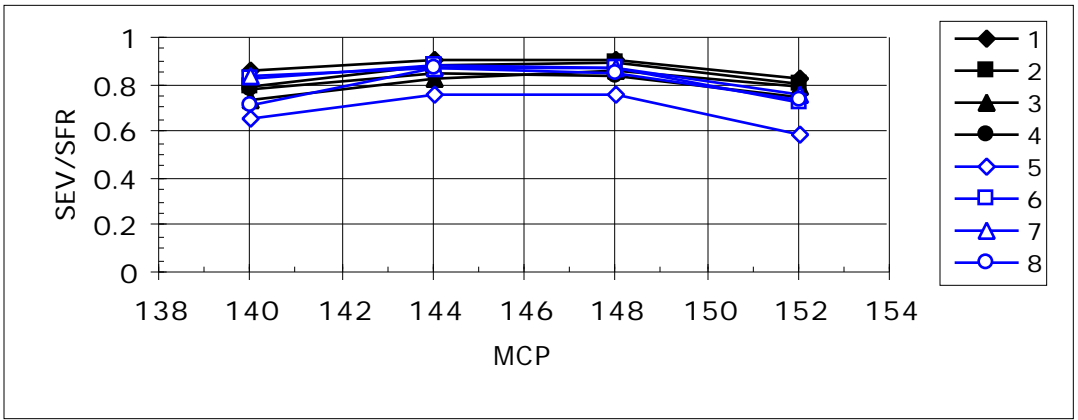


Figure 3: "Single Valid Event" efficiency versus MCP voltage for O+

Determining Ion Efficiencies vs. Energy

Once the optimum MCP voltage is set, data is collected at different beam energies. Figure 4 shows an example of the total ion efficiency (which is the product of the start, stop and valid event efficiencies) at optimum MCP voltage as a function of total ion energy (original beam energy plus post-acceleration). Even when the instrument is operating at the optimum MCP voltage, there is a significant difference between the final efficiencies measured at different positions (pixels). Thus it was necessary to determine the final ion efficiencies as a function not only of energy and species, but also of position. However, the position factor was not a strong function of energy so one multiplicative factor for each position and species was sufficient for normalization.

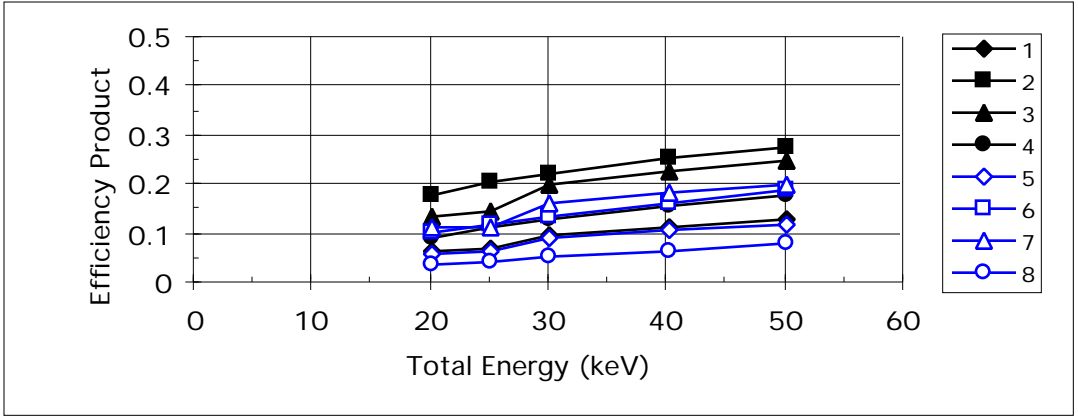


Figure 4: The total efficiency (product of SFR/PR, SFR/SF and SEV/SFR) versus Total Energy (beam energy plus PAC) for O+.

To normalize the data, an energy was chosen which had data for all pixels (i.e. for figure 4, 30 keV was used). Then the efficiency of each pixel at the chosen energy would be divided by a common factor, usually the average efficiencies of pixels 2 and 3. This gives the position factor to be multiplied with the other efficiencies. With the exception of protons, both sides (HS and LS) were adjusted to the same point.

Using these newly adjusted points, we fit a curve (a 2nd or 3rd order polynomial of the form $Y=M0+M1*X+M2*X^2+M3*X^3+M4*X^4$). Table 1, found after the N2+ section on P. 25, contains the polynomial parameters and multiplicative factors for each ion and figure 5 shows the results of multiplying the adjustment factors to the energies in each pixel and the curve that was fit to the adjusted points.

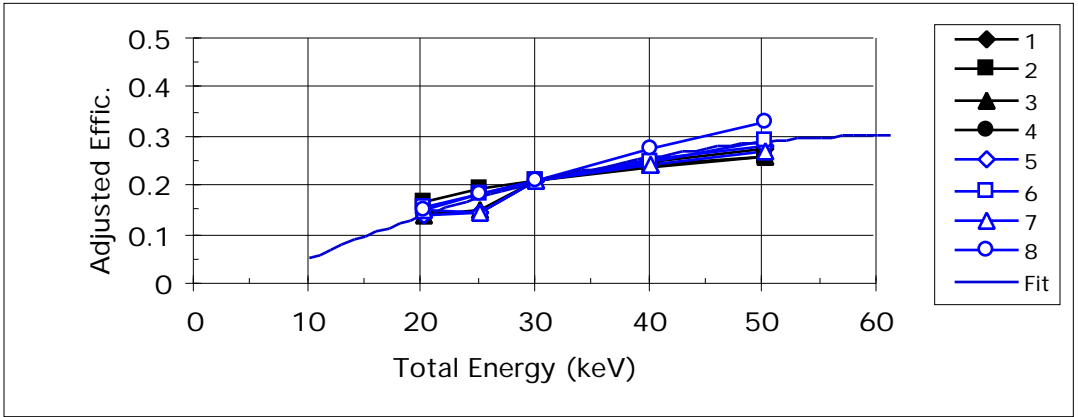


Figure 5: The total efficiency with pixel adjustment versus Total Energy for HS side O+.

Individual Ion Efficiencies:

Following are plots of the ion efficiencies versus total beam energy. Included are the plots of the “start” (SFR/PR), “stop” (SFR/SF), “valid event” (SEV/SFR), total and the adjusted total efficiency on both HS and LS for the O+, He+, He++, H+ and N2+ ions. The optimum efficiency used for all the ions is 94 hex or about 2.45 kV.

O+

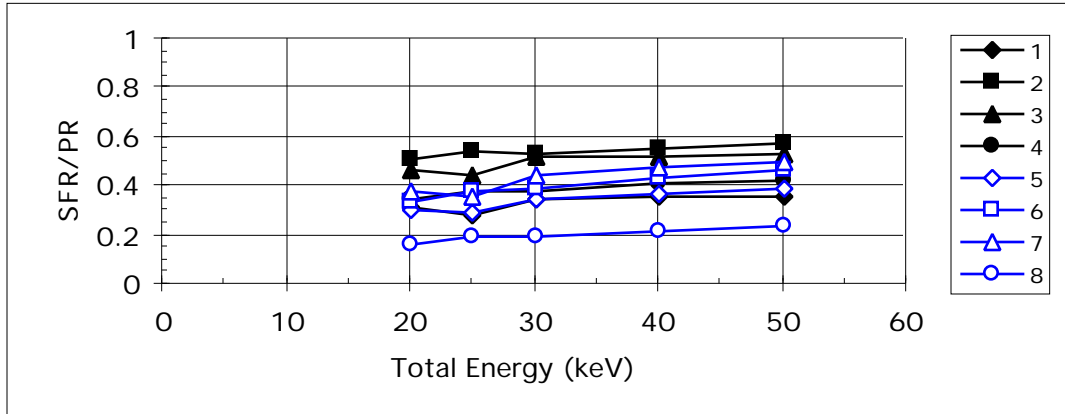


Figure 6a: HS side “Start” Efficiency versus Total Energy for O+.

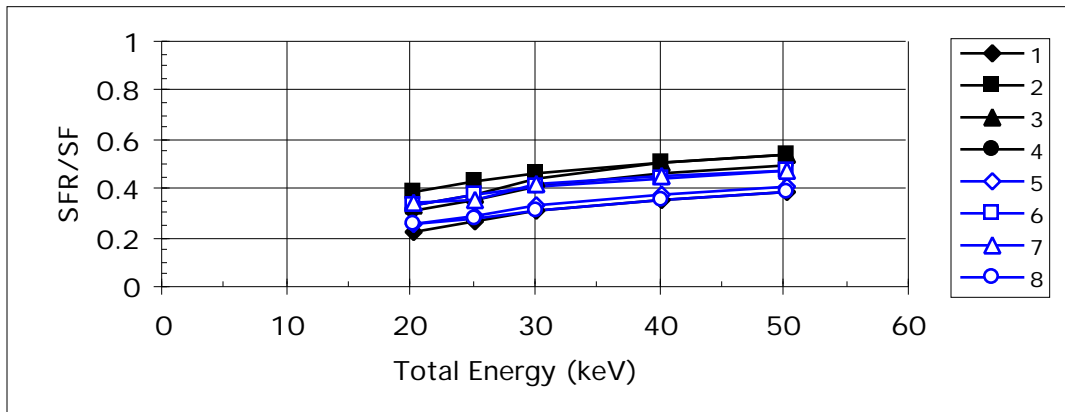


Figure 6b: HS side “Stop” Efficiency versus Total Energy for O+.

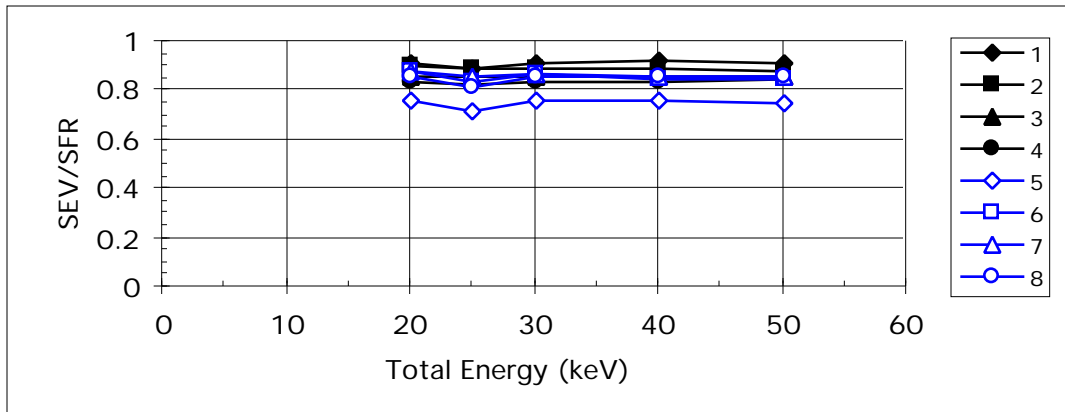


Figure 6c: HS side “Valid Event” Efficiency versus Total Energy for O+.

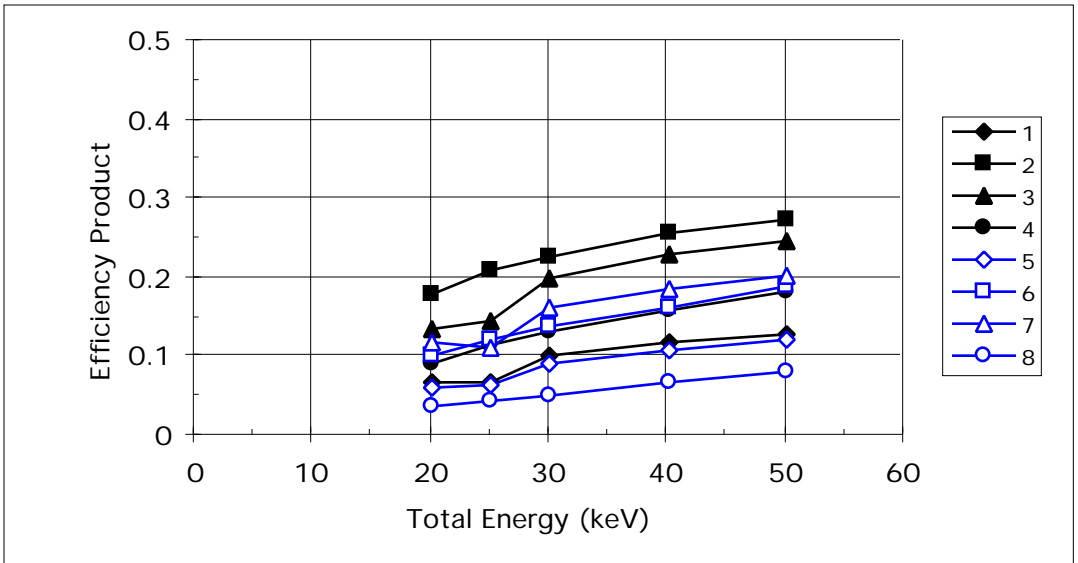


Figure 6d: HS side Total Efficiency versus Total Energy for O+.

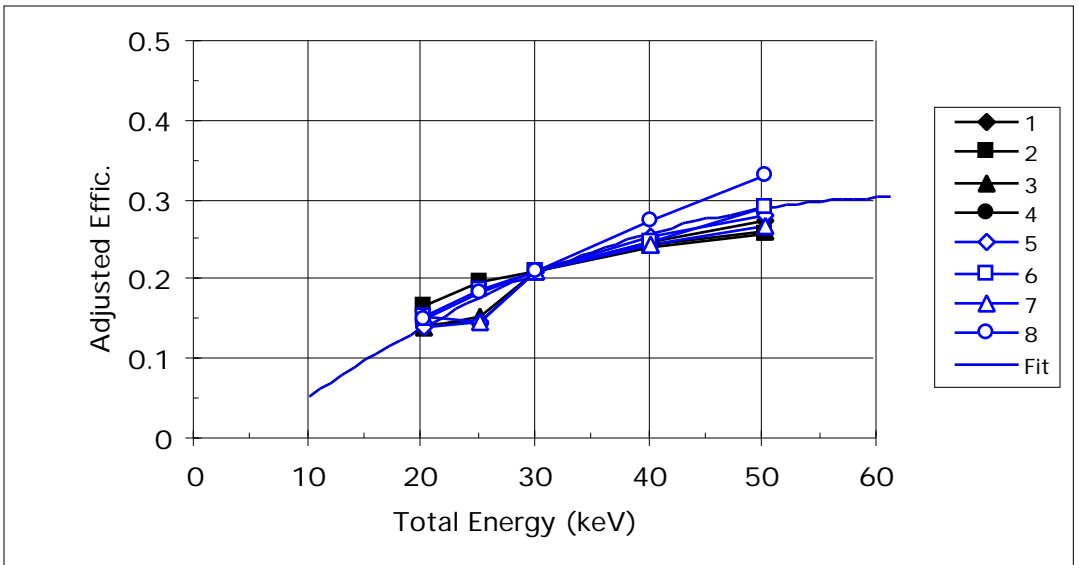


Figure 6e: HS side Total Efficiency w/ pixel adjustment versus Total Energy for O+.

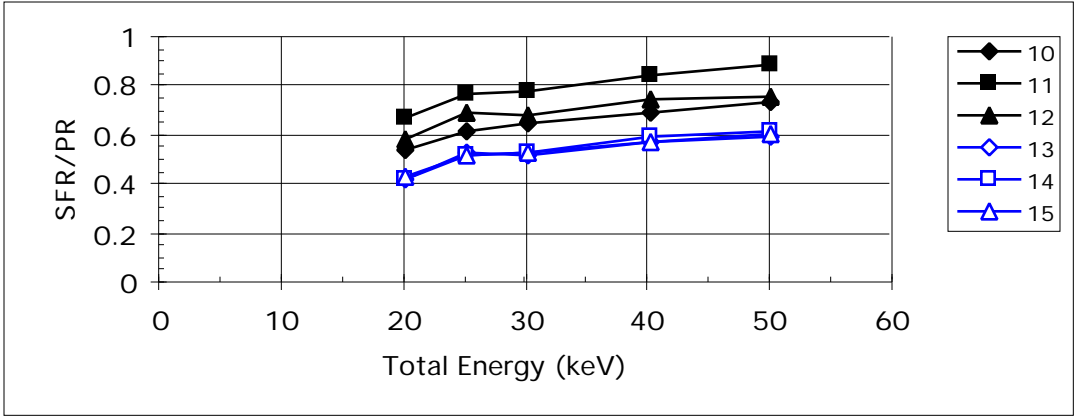


Figure 7a: LS side "Start" Efficiency versus Total Energy for O+.

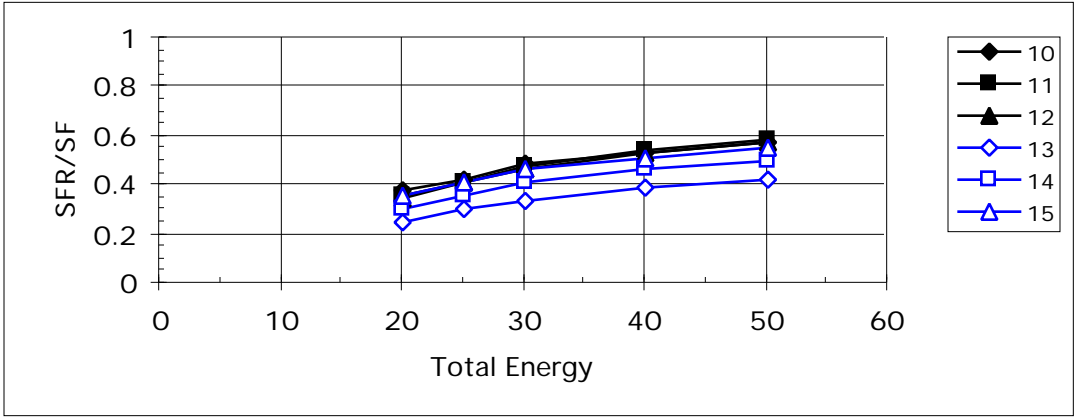


Figure 7b: LS side "Stop" Efficiency versus Total Energy for O+.

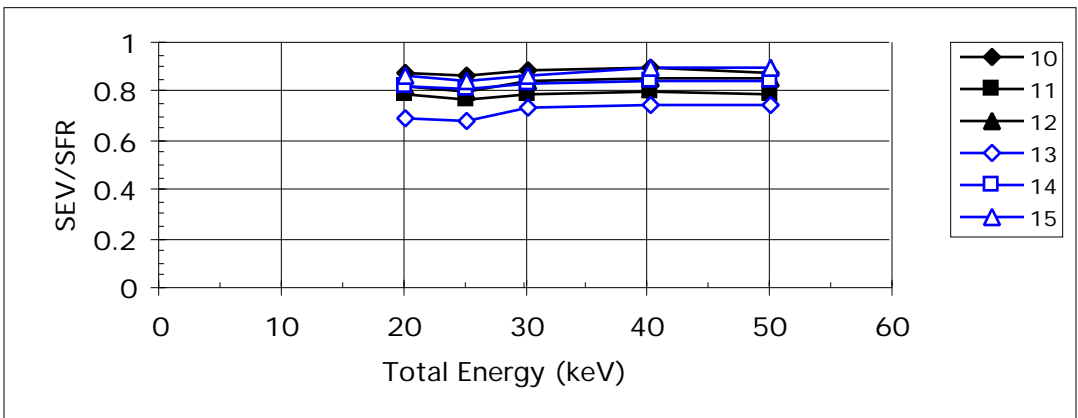


Figure 7c: LS side "Valid Event" Efficiency versus Total Energy for O+.

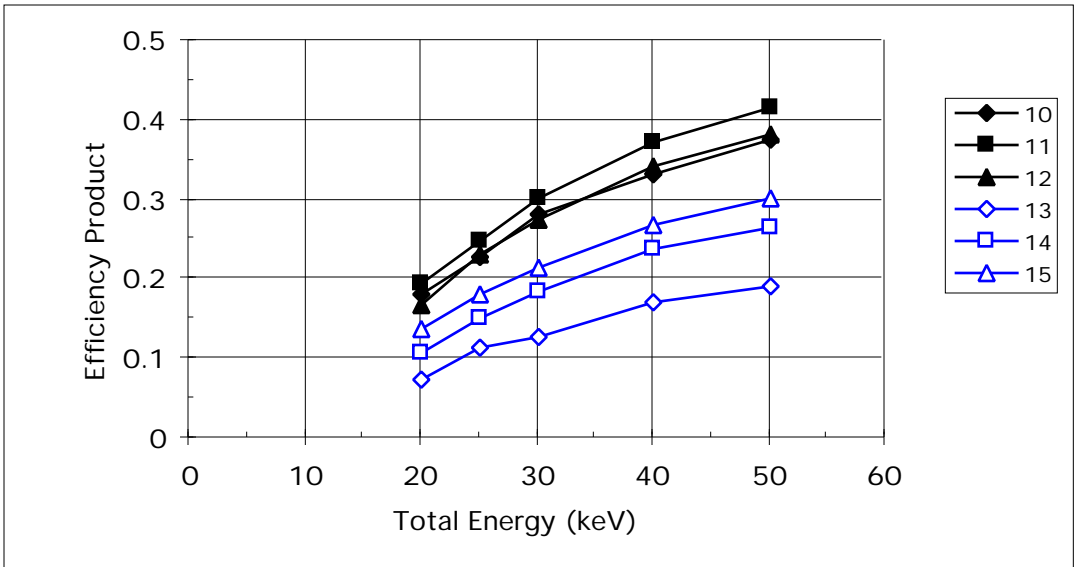


Figure 7d: LS side Total Efficiency versus Total Energy for O+.

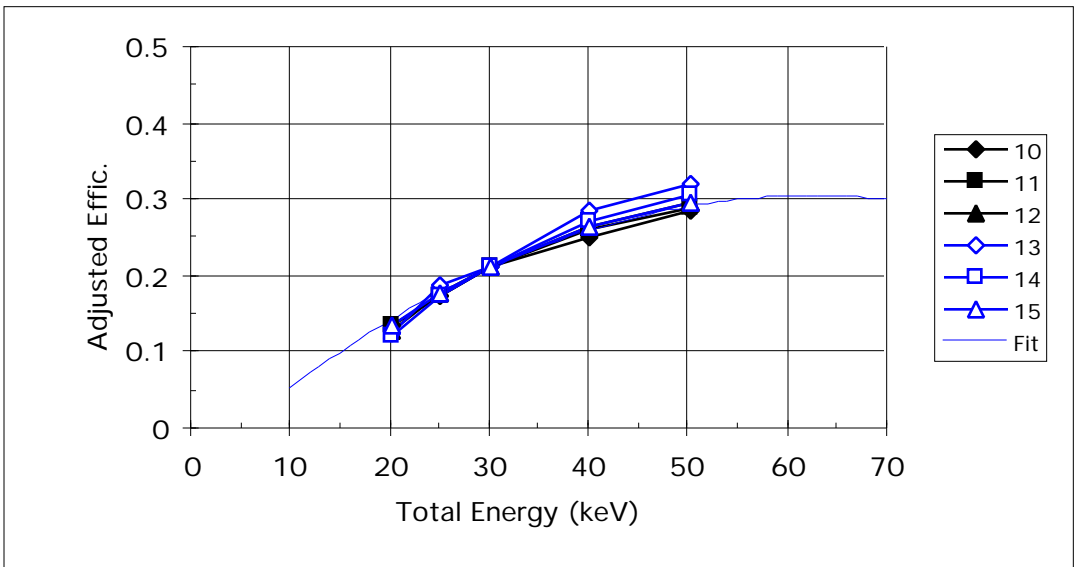


Figure 7e: LS side Total Efficiency w/ pixel adjustment versus Total Energy for O+.

He+

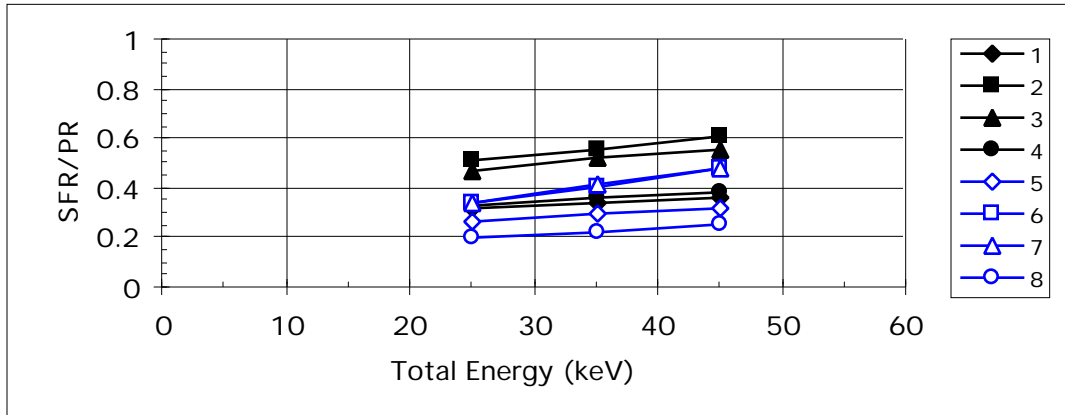


Figure 8a: HS side “Start” Efficiency versus Total Energy for He+.

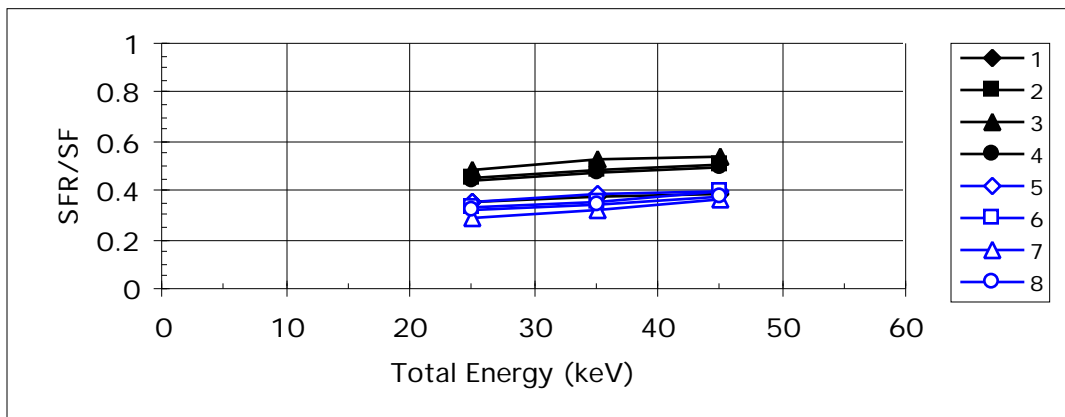


Figure 8b: HS side “Stop” Efficiency versus Total Energy for He+.

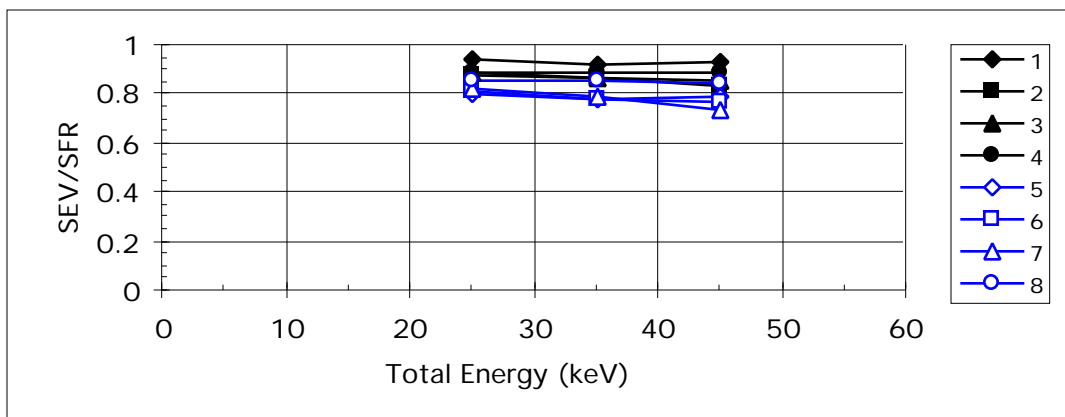


Figure 8c: HS side “Valid Event” Efficiency versus Total Energy for He+.

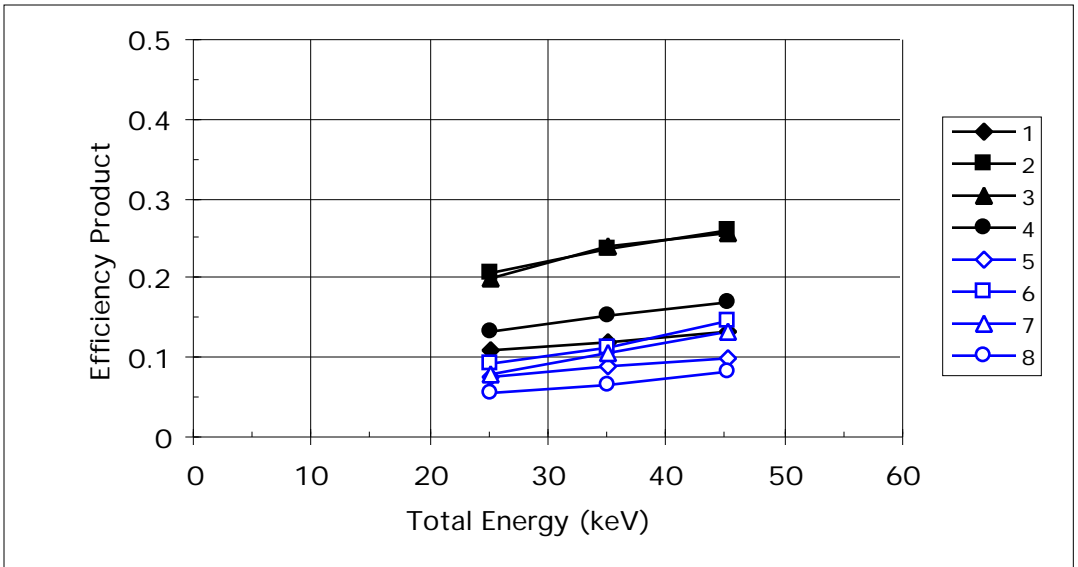


Figure 8d: HS side Total Efficiency verses Total Energy for He+.

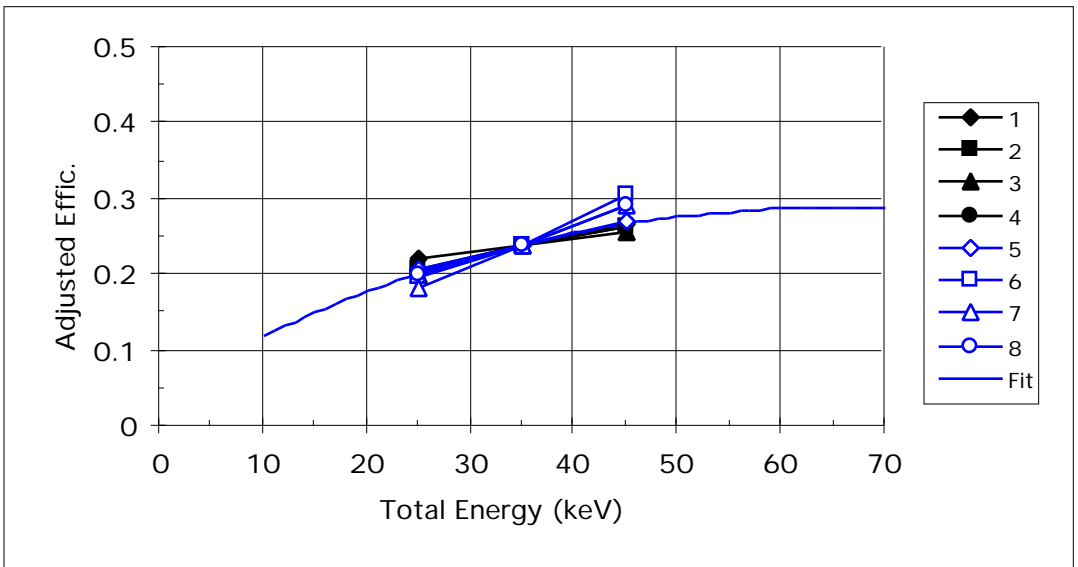


Figure 8e: HS side Total Efficiency w/ pixel adjustment verses Total Energy He+.

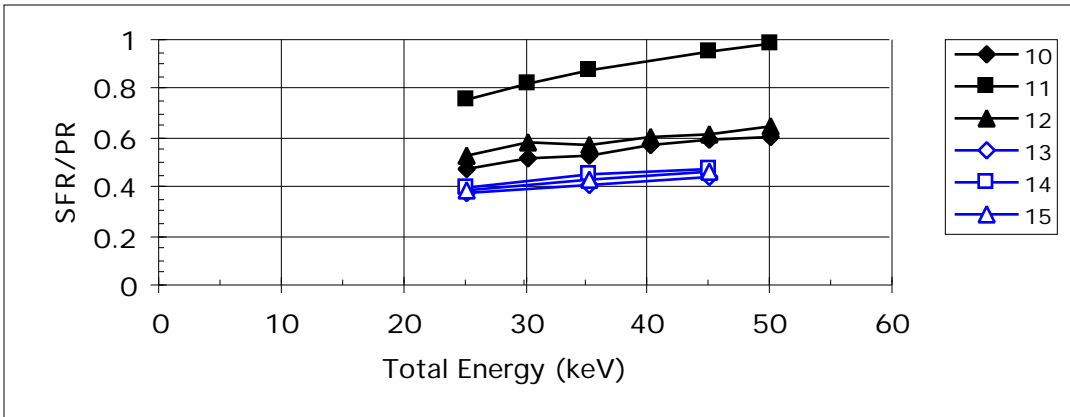


Figure 9a: LS side "Start" Efficiency versus Total Energy for He+.

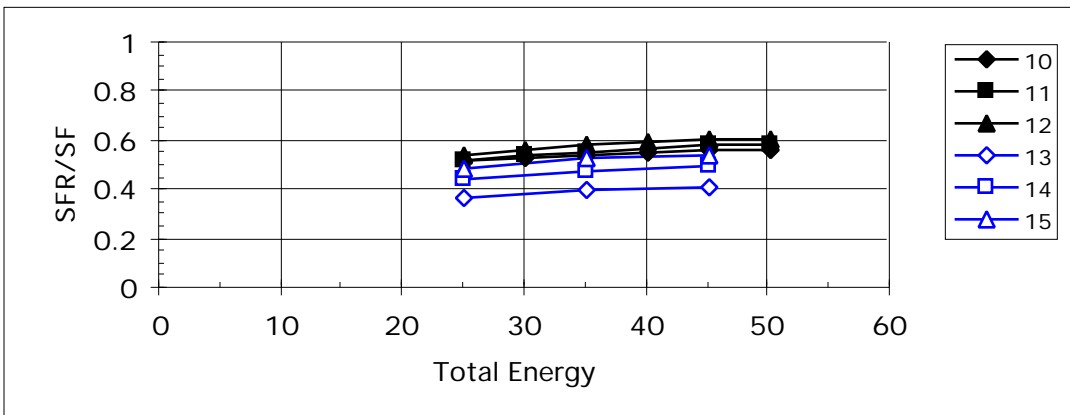


Figure 9b: LS side "Stop" Efficiency versus Total Energy for He+.

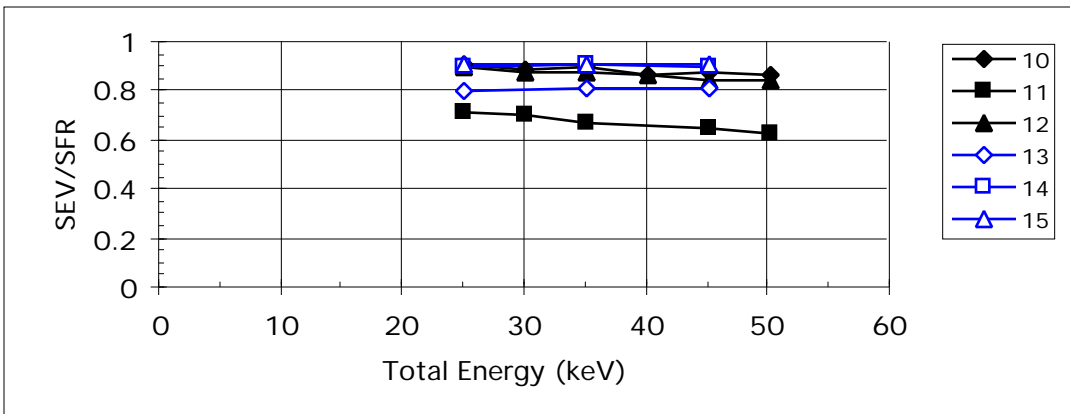


Figure 9c: LS side "Valid Event" Efficiency versus Total Energy for He+.

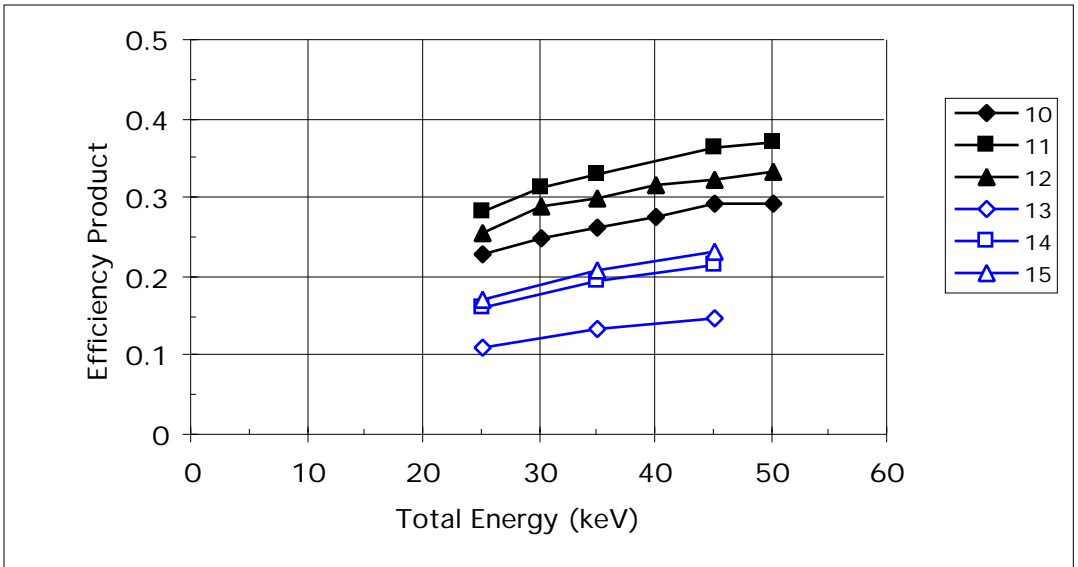


Figure 9d: LS side Total Efficiency versus Total Energy for He+.

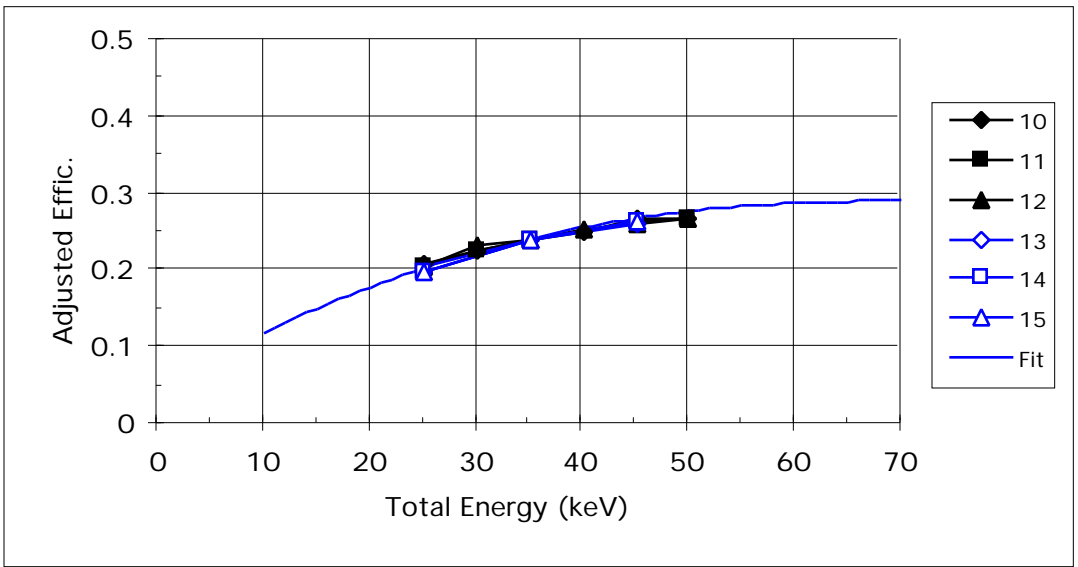


Figure 9e: LS side Total Efficiency w/ pixel adjustment versus Total Energy for He+.

He⁺⁺

He⁺ and He⁺⁺ have the same efficiencies at the same total energy. Therefore, the same position factors are used for the two. However, the best fit to the He⁺ data over the energies up to 65 keV begins to increase at higher energies. Therefore, we fit a separate curve for the He⁺⁺ data which remains flat out to 120 keV. The He⁺⁺ curve is shown below.

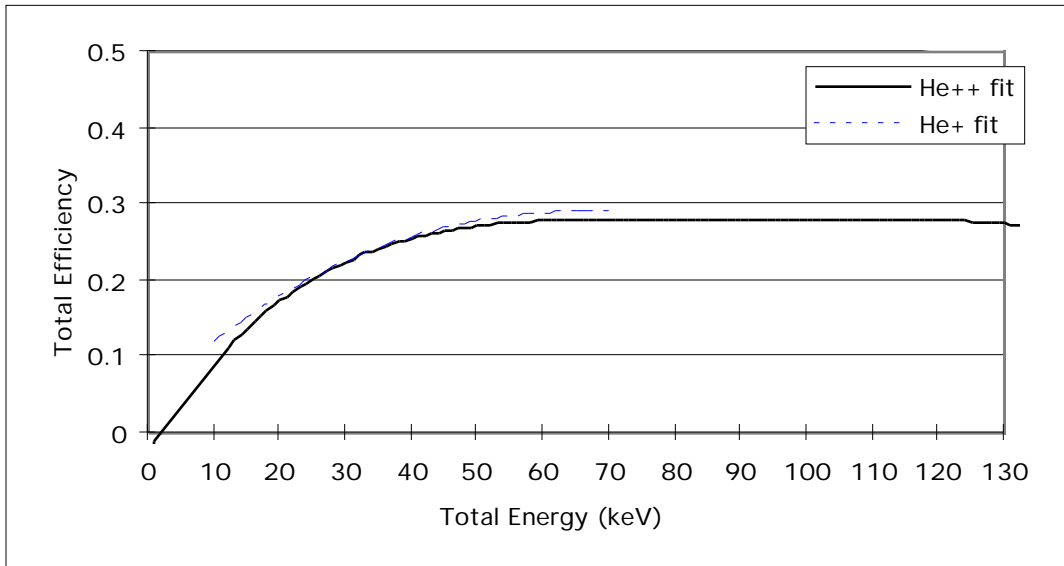


Figure 10: He⁺ and He⁺⁺, calibration curves shown to 130 keV.

H⁺

The Hydrogen ion has the worst efficiency and the least consistent efficiency curve of all the ions. The problem is that when the MCP's are operating at a voltage that is optimum for the other ions, the efficiency for H⁺ has not yet reached a plateau. This leads to a much lower efficiencies, particularly at high energies and to much greater variations between the pixels. We think that the stop efficiency is particularly low. We attempted to improve the stop efficiency by exchanging a grid that determines the split of signals between the "stop" rate and the "stop position" rate, PR. This did improve the efficiencies, particularly on the LS side, but they are still not as good as the other ion species. The best fits to the efficiency curves are significantly different on the HS and LS sides. We performed fits to both sides, but since only one curve can be input into the DPU, the HS curve is currently used.

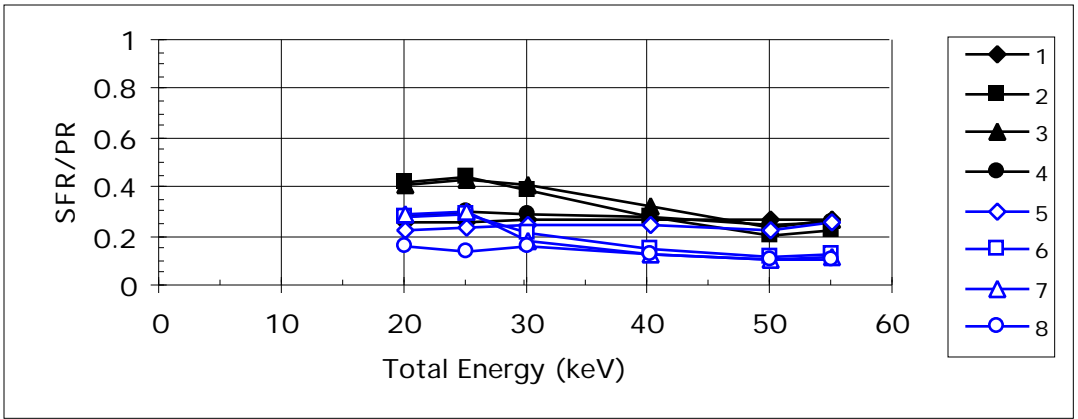


Figure 11a: HS side “Start” Efficiency versus Total Energy for H+.

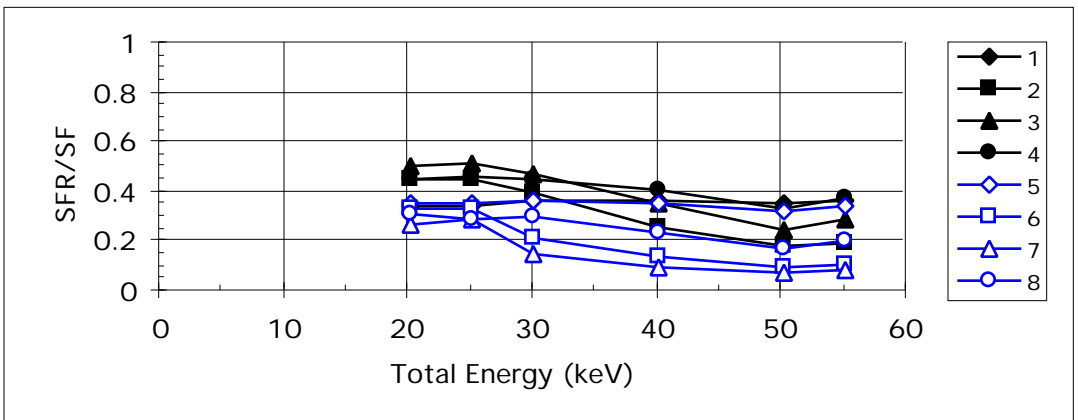


Figure 11b: HS side “Stop” Efficiency versus Total Energy for H+.

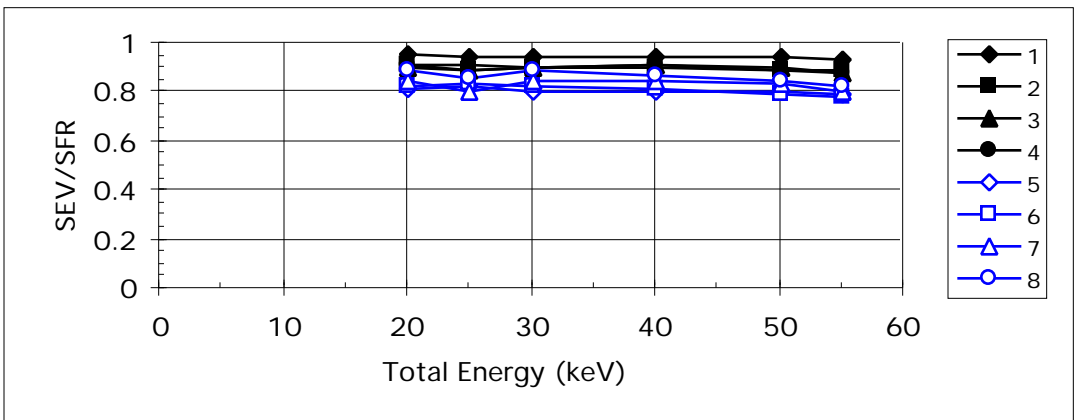


Figure 11c: HS side “Valid Event” Efficiency versus Total Energy for H+.

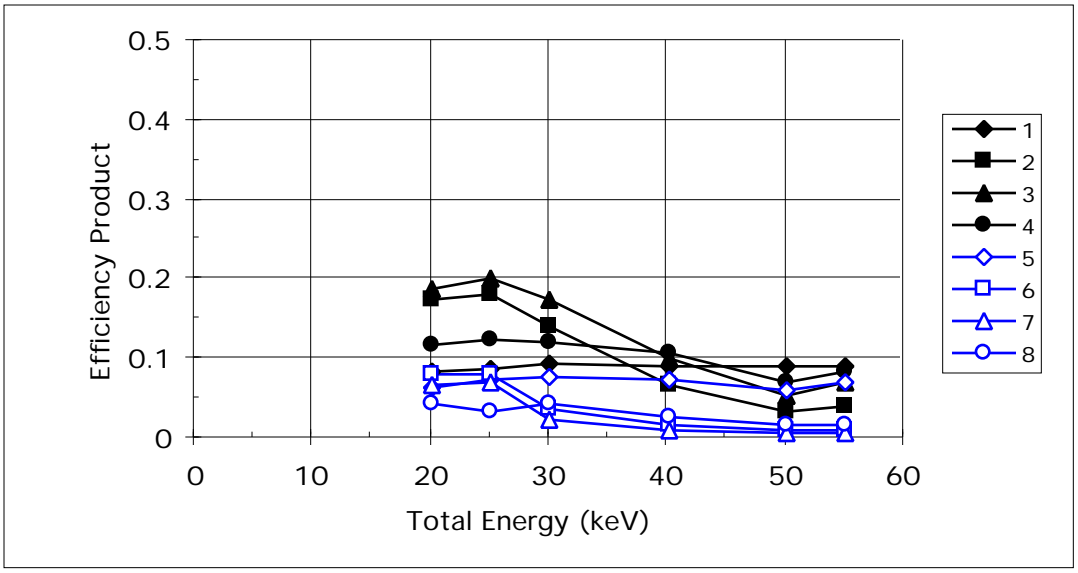


Figure 11d: HS side Total Efficiency versus Total Energy for H+.

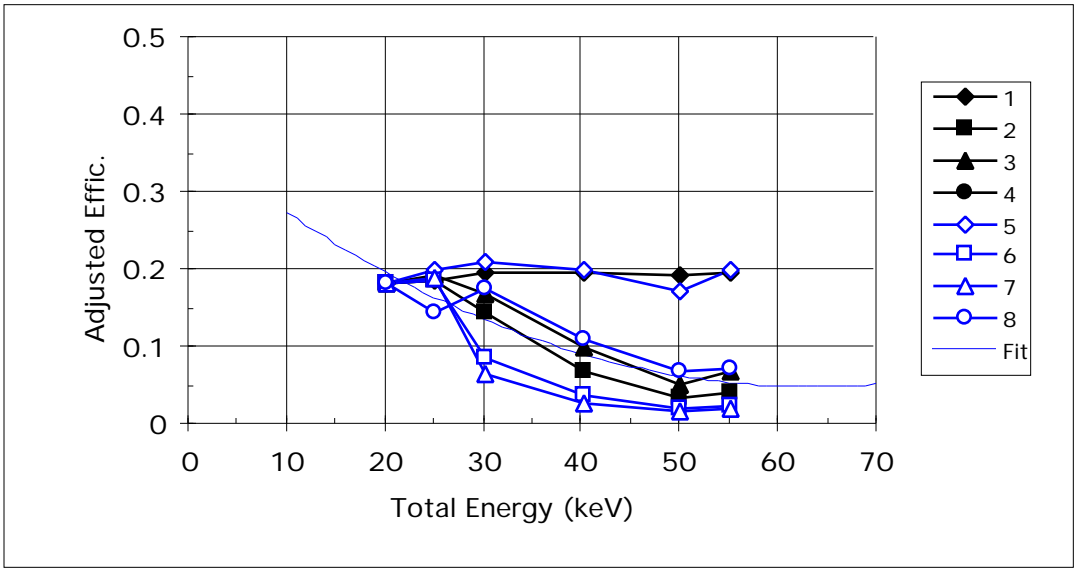


Figure 11e: HS side Total Efficiency w/ pixel adjustment versus Total Energy H+.

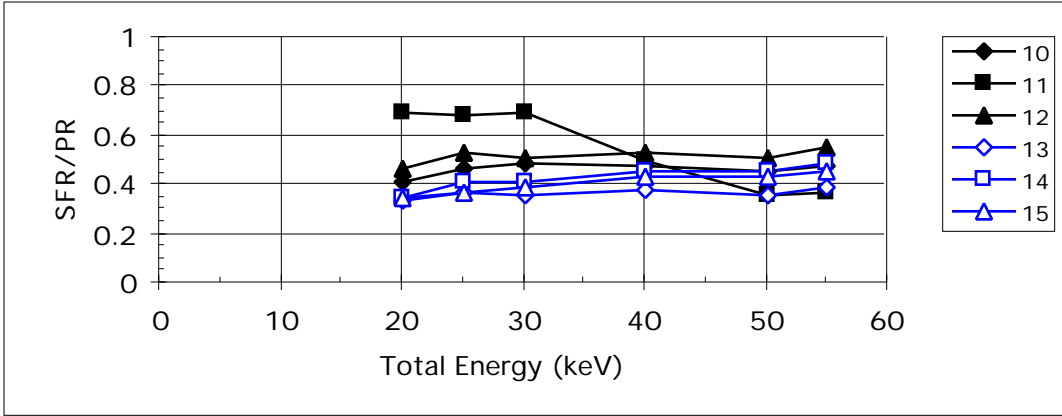


Figure 12a: LS side "Start" Efficiency versus Total Energy for H+.

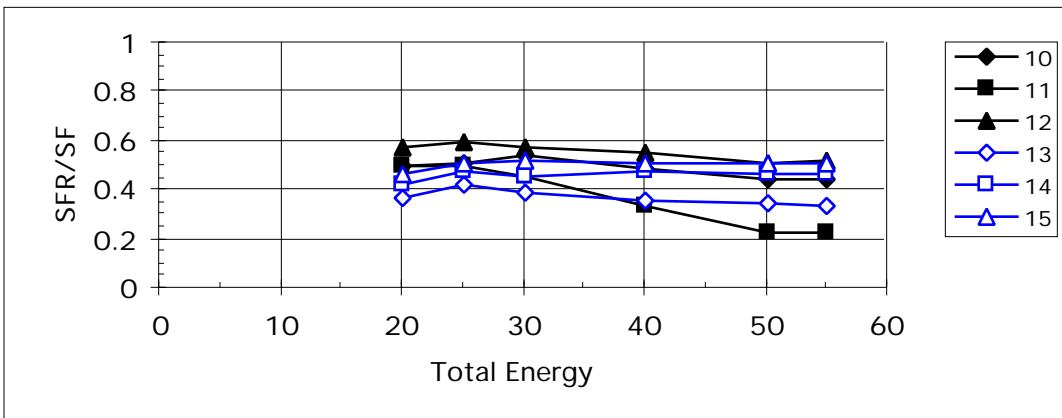


Figure 12b: LS side "Stop" Efficiency versus Total Energy for H+.

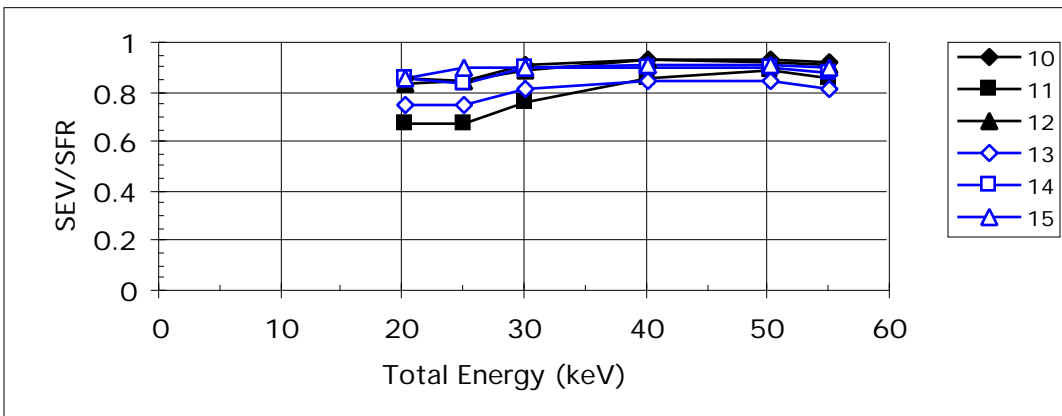


Figure 12c: LS side "Valid Event" Efficiency versus Total Energy for H+.

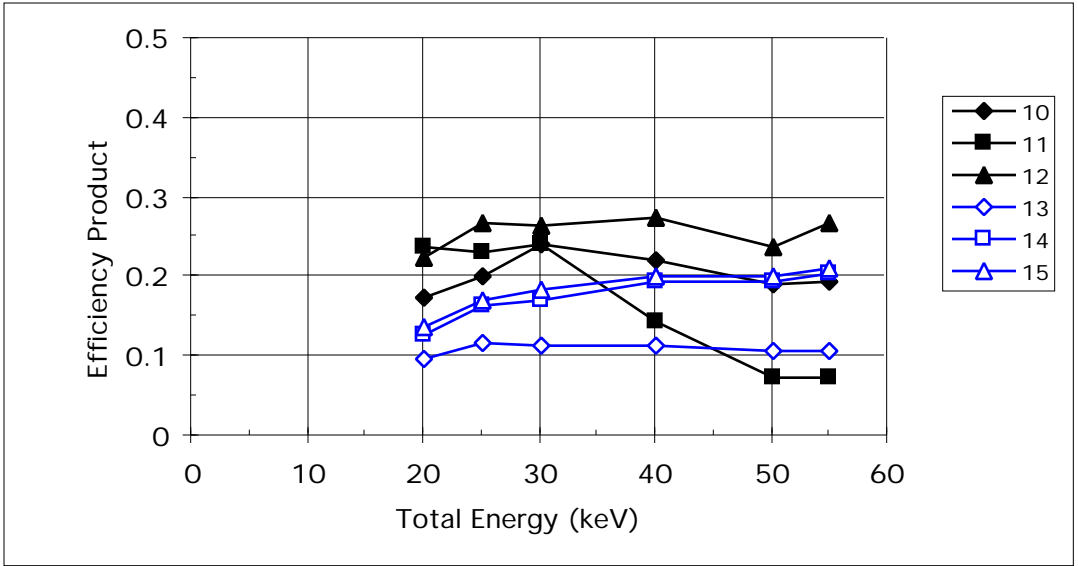


Figure 12d: LS side Total Efficiency versus Total Energy for H+.

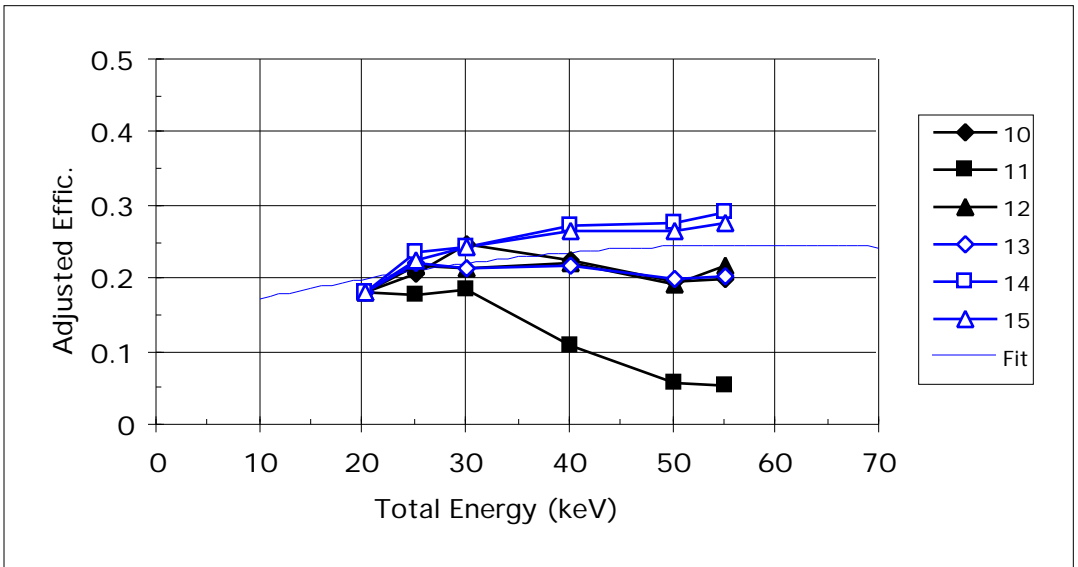


Figure 12e: LS side Total Efficiency w/ pixel adjustment versus Total Energy for H+.

N2+

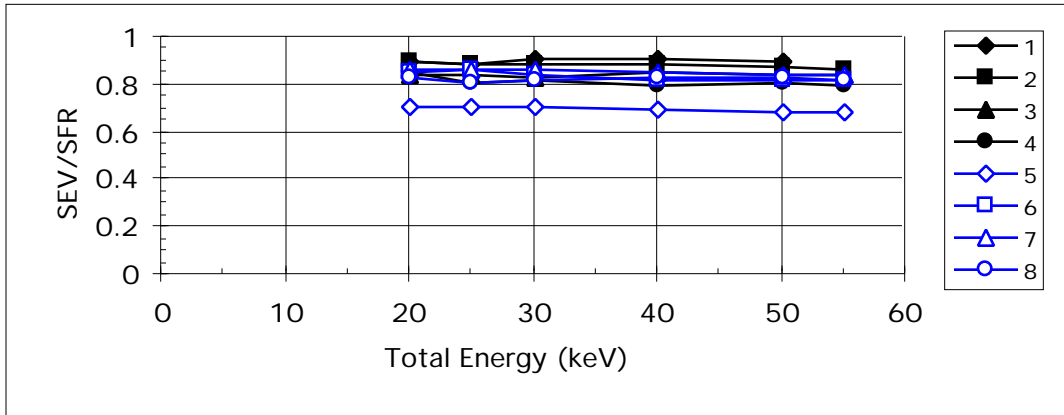


Figure 13a: HS side “Start” Efficiency versus Total Energy for N2+.

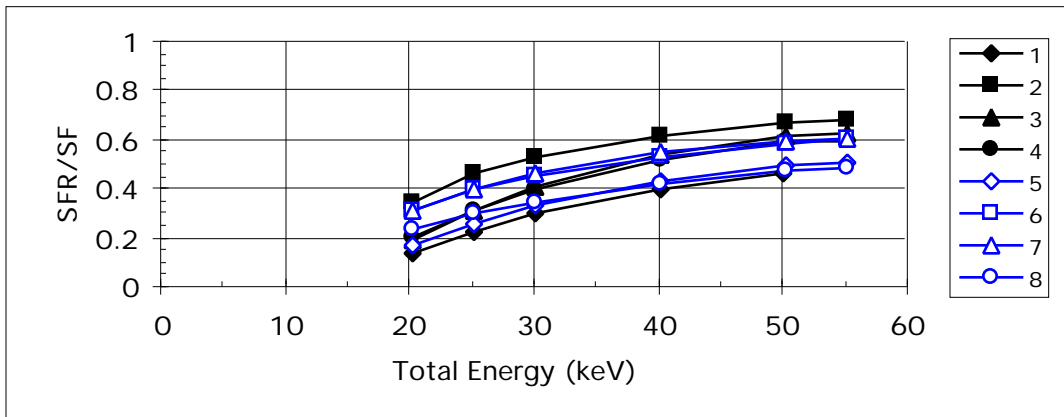


Figure 13b: HS side “Stop” Efficiency versus Total Energy for N2+.

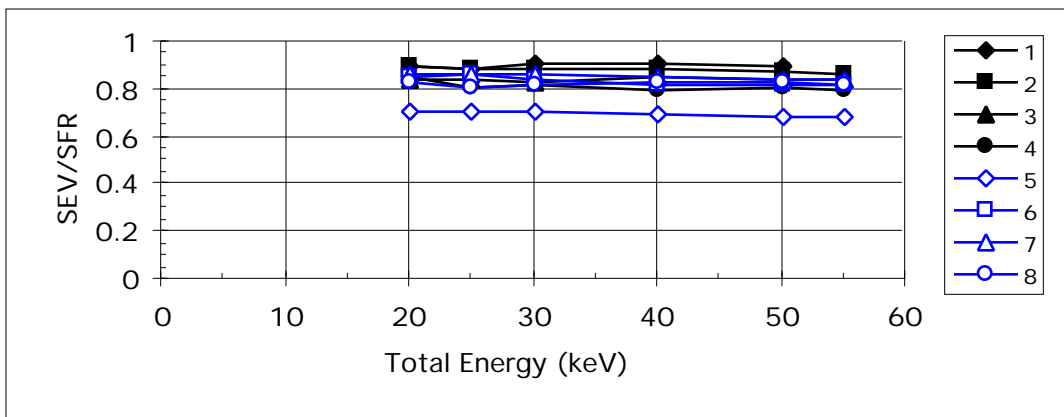


Figure 13c: HS side “Valid Event” Efficiency versus Total Energy for N2+.

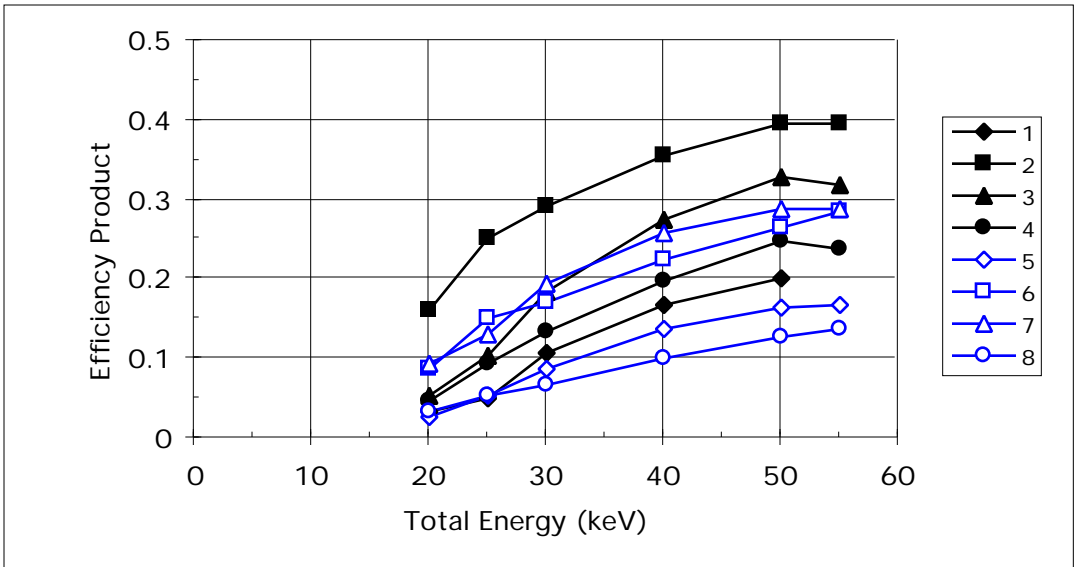


Figure 13d: HS side Total Efficiency versus Total Energy for N2+.

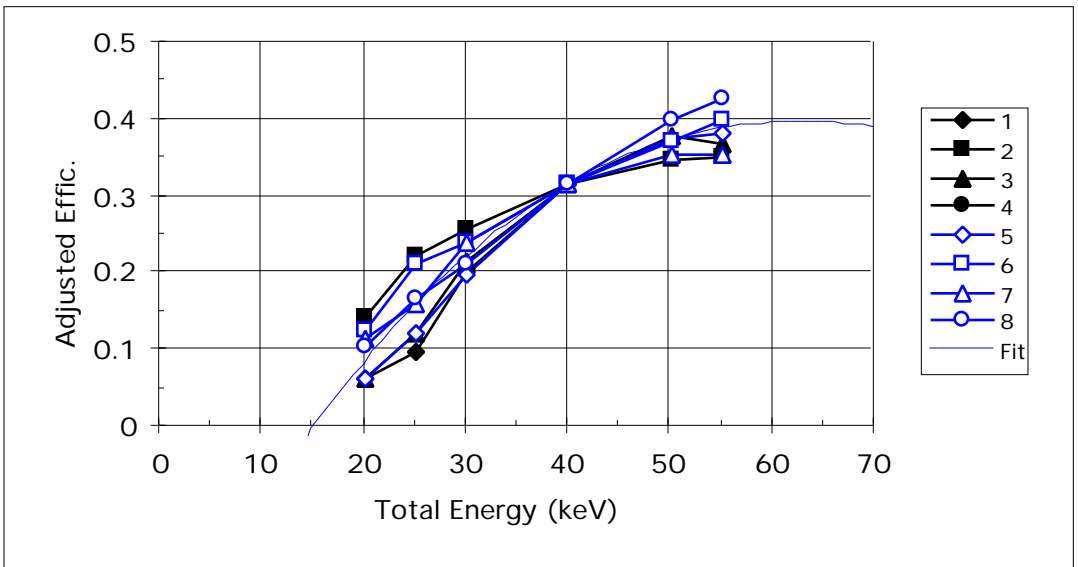


Figure 13e: HS side Total Efficiency w/ pixel adjustment versus Total Energy for N2+.

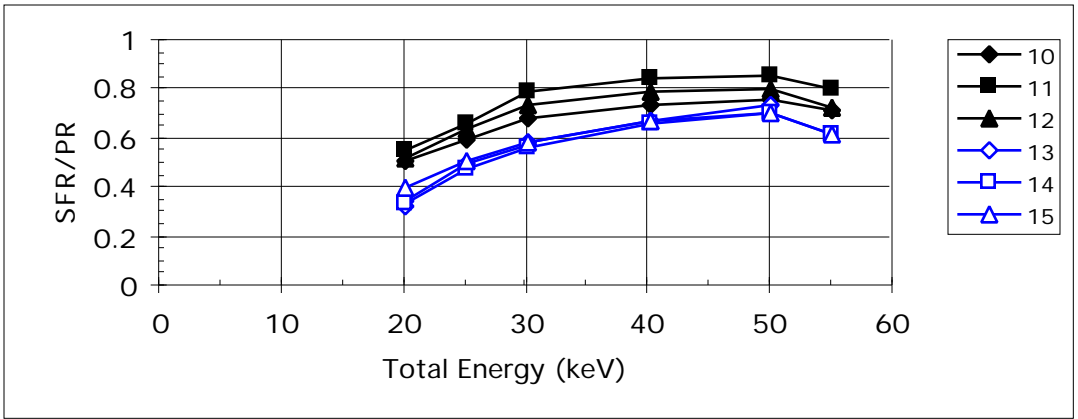


Figure 14a: LS side “Start” Efficiency versus Total Energy for N2+.

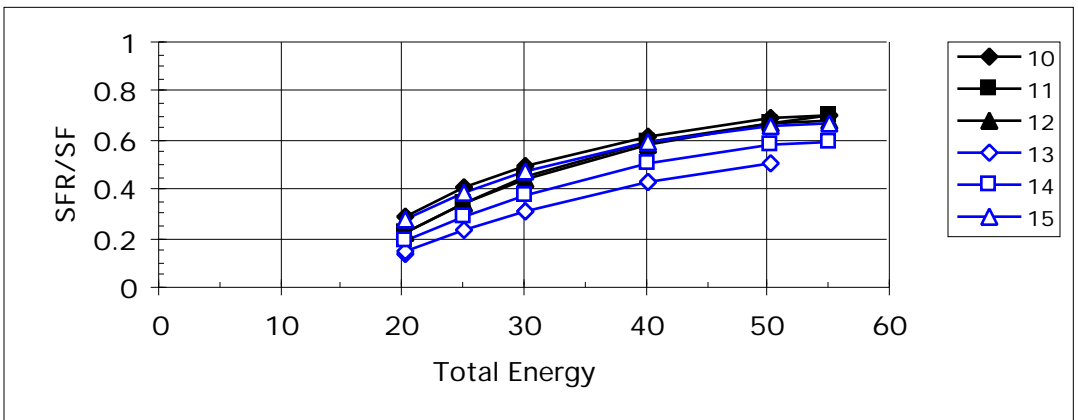


Figure 14b: LS side “Stop” Efficiency versus Total Energy for N2+.

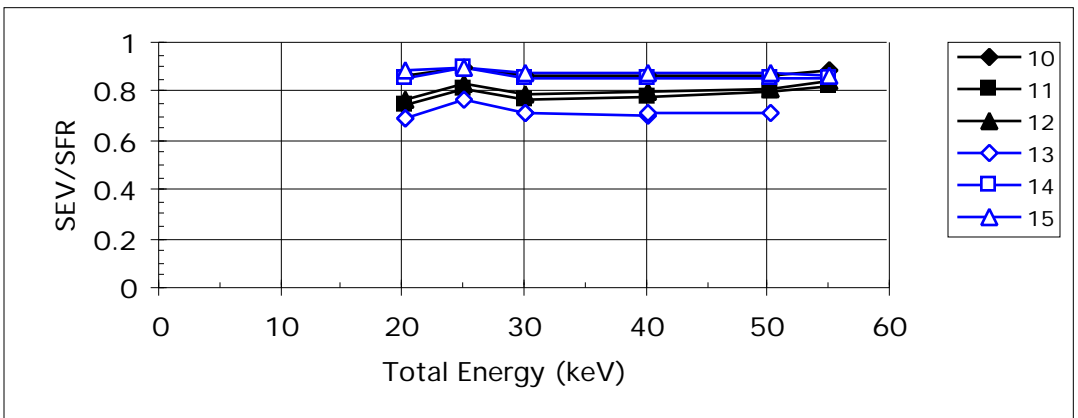


Figure 14c: LS side “Valid Event” Efficiency versus Total Energy for N2+.

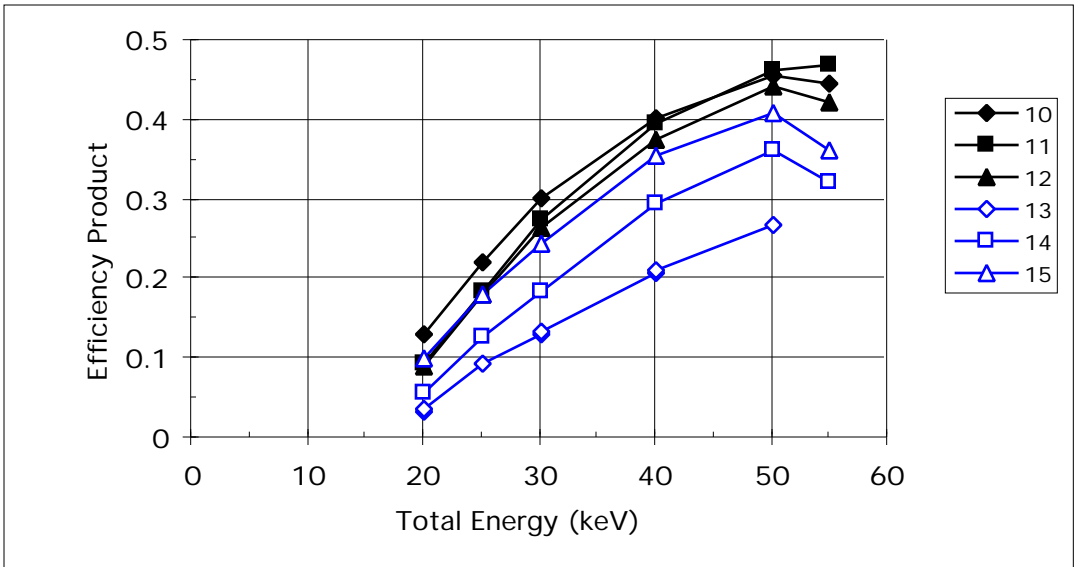


Figure 14d: LS side Total Efficiency versus Total Energy for N2+.

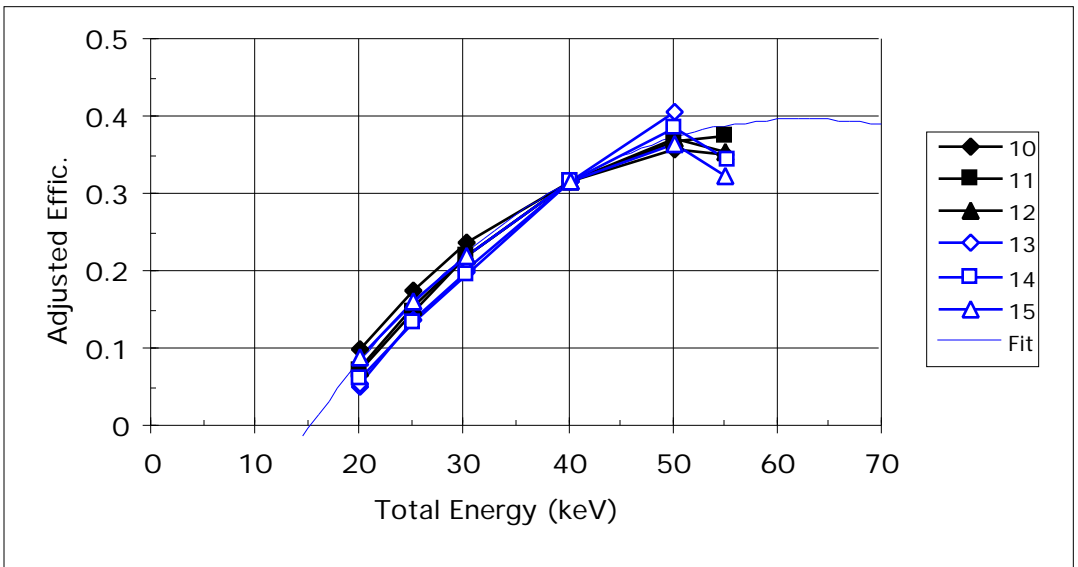


Figure 14e: LS side Total Efficiency w/ pixel adjustment versus Total Energy for N2+.

Ions	O+	N2+	He+	He++	H+ (HS side)	H+ (LS side)
M0	-5.4001E-02	-3.3954E-01	4.5858E-02	-2.3741E-02	3.6445E-01	1.3712E-01
M1	1.1658E-02	2.6319E-02	8.1530E-03	1.3875E-02	-1.0010E-02	3.7095E-03
M2	-9.7951E-05	-2.7849E-04	-80854E-05	-2.3346E-04	7.8932E-05	-3.1570E-05
M3	5.2118E-08	7.3138E-07	2.0281E-07	1.7167E-06	-	-
M4	-	-	-	-4.6605E-09	-	-
PF1	2.134	1.865	1.990		2.132	
PF2	0.945	0.883	1.008		1.033	
PF3	1.062	1.152	0.992		0.969	
PF4	1.614	1.596	1.542		1.539	
PF5	2.337	2.292	2.662		2.786	
PF6	1.542	1.407	2.076		2.278	
PF7	1.322	1.219	2.209		2.706	
PF8	4.110	3.108	3.504		4.149	
PF10	0.759	0.786	0.909		1.031	
PF11	0.703	0.798	0.721		0.766	
PF12	0.777	0.843	0.798		0.811	
PF13	1.681	1.508	1.758		1.892	
PF14	1.148	1.070	1.220		1.423	
PF15	0.991	0.891	1.138		1.318	

Table 1: Efficiency curve polynomials and adjustment factors for each ion..

ESA/Alpha Acceptance

Given a fixed beam energy, the ESA/alpha files demonstrates the acceptance range of particles over changing ESA voltages and azimuthal entrance degrees. Figure 15 is an example of the plot from an ESA/alpha file.

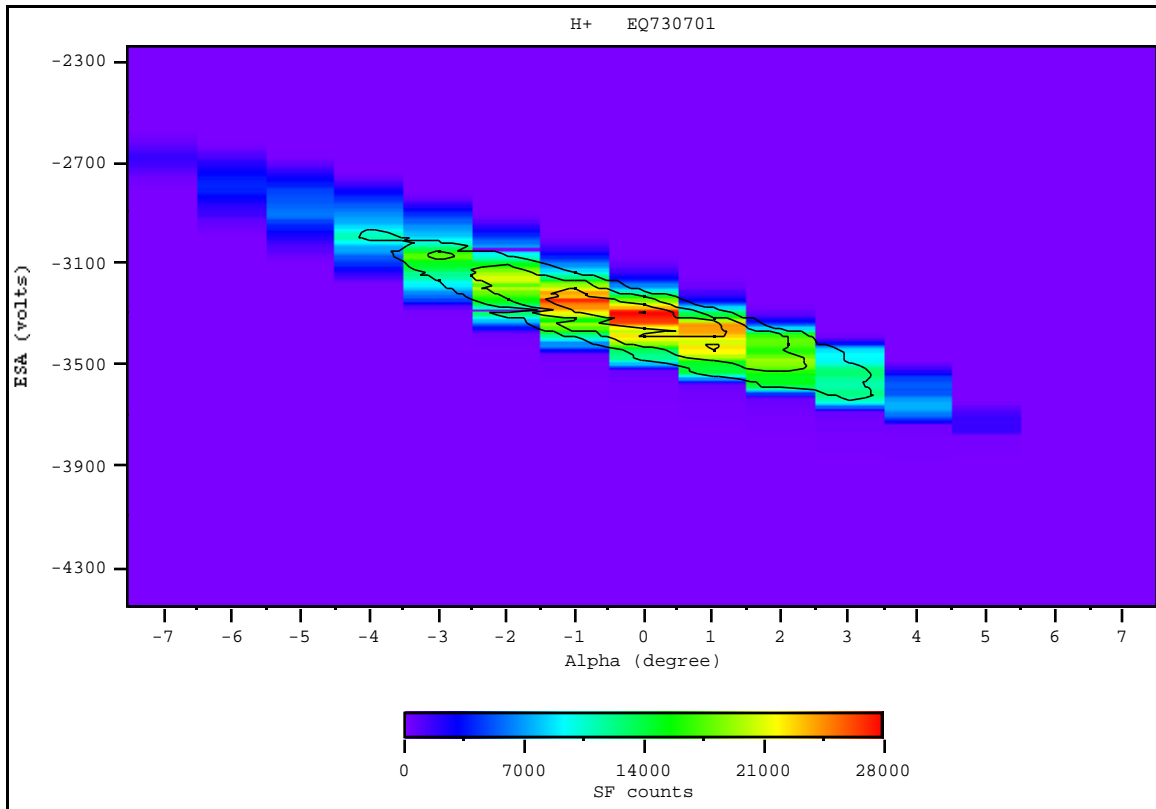


Figure 15: ESA/alpha plot for protons with total energy 55 keV.

The ESA/alpha data is used to determine the energy and angle acceptance range of the analyzer, and to get the geometric factor. To get ranges the 2D matrix is summed over the full angular range to get the energy acceptance and over the full energy range to get the angular acceptance. Then a gaussian curve with a linear background (of the form $y=a+b*\exp[-((x-c)/d)^2]$) is fit to the points. Figure 16 shows the above ESA/alpha plot condensed onto the ESA axis. Figure 17 shows the above ESA/alpha plot condensed onto the alpha axis.

The expected peak ESA voltage depends on the beam energy, however, the expected peak alpha is zero.

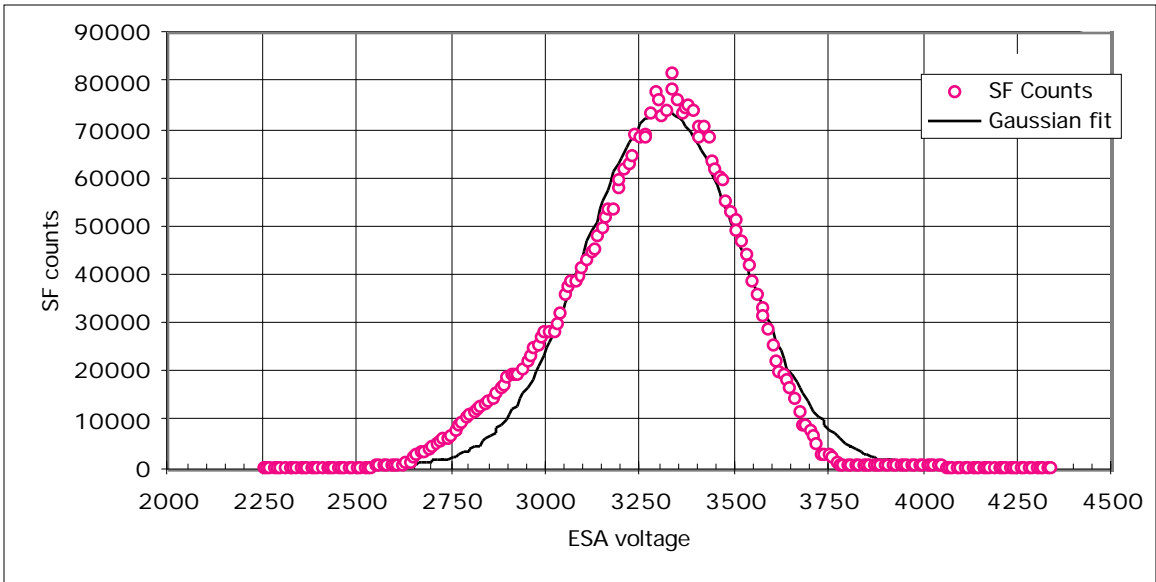


Figure 16: Alpha angles summed for each ESA voltage for the proton with total energy 55 keV.

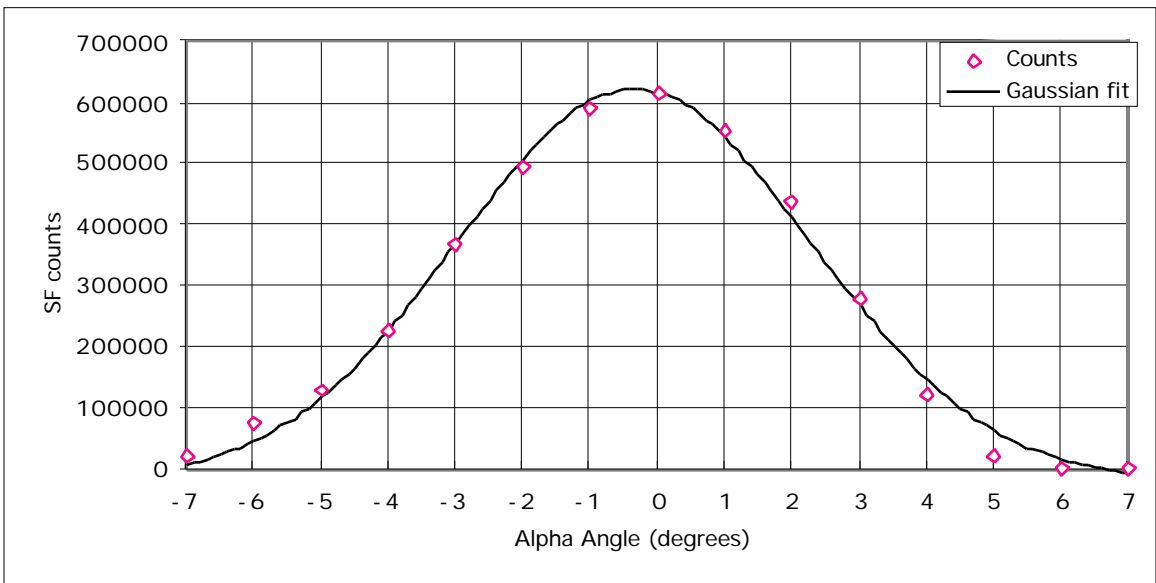


Figure 17: ESA voltages summed for each Alpha angle for the proton with total energy 55 keV.

For each ion in the Bern '97 calibration, Table 2 gives the peak ESA voltage, peak Alpha angle and fwhm of these values. Also given is the k constant. As the beam energy of the incoming particles change, the ESA voltage must be changed accordingly to

maximize the counts entering the CODIF. The beam energy and peak ESA have a linear relationship and the slope between them is defined as the analyzer constant, k.

$$\text{Ion Beam Energy} = k * \text{peak ESA voltage}$$

The analyzer constant is used in calculating the geometric factor (See geometric factor section). The beam energy is a predetermined value given to the incoming particles. The peak ESA voltage (summed over alpha degrees, see figure 16 above) is calculated from ESA/Alpha files.

Ion	pixel	Ion Beam Energy keV	ESA peak volts	ESA fwhm	fwhm	k constant	Alpha peak degrees	Alpha fwhm
					peak			
H+	7	25	3309	495	0.150	7.56	-0.50	6.50
H+	3	25	3309	489	0.148	7.56	-0.35	6.22
He+	6	5	662	93	0.140	7.55	-0.32	6.17
He+	2	5	671	96	0.144	7.46	-0.20	6.17
O+	7	25	3322	489	0.147	7.53	-0.19	6.08
N2+	11	25	3303	477	0.144	7.57	-0.12	6.08
N2+	3	25	3315	477	0.144	7.54	-0.26	5.99

Table 2: Equator-S Bern '97 calibration, .

The average k for this calibration is 7.54. Viewing other calibration sets, it is seen that the k factor is generally 7.5 so this is the accepted value when using the k factor in calculations.

The geometric factor calculation also use the summed SF rate and start efficiency from the ESA/alpha file for the particle flux calculations.

Geometric Factor

In order to accept a large range of particle flux, CODIF is divided into two sections. One half is the HS side (High Sensitivity), pixels 1-8, and the other is the LS side (Low Sensitivity), pixels 10-15. Pixels 9 and 16 are blocked by support structures. Grids to attenuate the incident particles are placed at the entrance of the ESA which leads to the LS side of the instrument. It is expected that these grids will cause the ion flux to be about 100 times smaller on the LS side than the HS side. A measure of the ion flux is the geometric factor which is the ratio of the ion flux at the entrance of the ESA (electrostatic analyzer) to the number of ions that exit the ESA.

Geometric Factor Calculation

If we have a flux of j (cts/(cm²-ster-keV/e)) at the instrument entrance, and a count rate of N (cts/s) is measured in the instrument, the geometric factor, G is defined as $G = N/j$, with units (cm² - ster - keV)

The effective incoming "omni-direction flux" j is

$$j = (dN/ dt) * 1 / (dE dA d)$$

Incoming beam rate: dN/ dt ct/s is recorded from the CEM beam monitor

Change in beam energy $dE = \Delta E$ with units (KeV)

= 7.5 (see ESA/alpha section above)

$d(ESA) =$ ESA step size volts (usually between 2 and 10 volts)

beam monitor area: $dA = 0.1$ cm²

solid angle step size: $d\Omega = 22.5$ degrees * 1 degree = 0.006854 radians

For the count rate N (cnts/s), the start rate (SF) is summed over all the ESA/Alpha steps. Since the SF rate does not count all the particles entering the instrument, it is divided by the start efficiency (SFR/PR) which tells of the percentage of incoming particle that are actually counted. (i.e. If SF = 100 and the start efficiency is 50%, then there were actually 200 particles that entered the instrument) For consistency the background counts were subtracted from all files. For files where the background was a significant contributor to the overall rates, subtracting it did make a difference in the geometric factor.

$N = (SF) / (SFR/PR)$ with units of cnts/s.

Since the geometric factor depends on the incoming energy, an energy independent factor, g , can be found by dividing G by the energy E (keV) of the incoming beam.

$g = G/E$ with units (cm²-ster)

Geometric Factor Conclusions:

The geometric factor (g.f.) for the Cluster CODIF instruments are on Table 3 below. As was said above, the target ratio for the HS geometric factor over the LS is one hundred. Since the g.f. on the LS side of the first instrument (FS) was too high the grids covering the LS side were adjusted to reduce the particles entering the instrument. Subsequent instruments were closer to the 100 HS/LS geometric factor ratio with the only remaining CODIF instrument (F4) having the best g.f. HS/LS ratio.

Cluster	HS side	LS side
FS	2.51E-03	5.40E-05
F1	2.01E-03	3.26E-05
F2	2.38E-03	2.30E-05
F3	2.30E-03	N/A
F4*	2.20E-3	2.17E-05

*The F4 model later became the flight spare (FS) since it was the only CODIF instrument not “launched”
 Table 3: Geometric factors for the different Cluster models

Table 4 shows the geometric factors for the Bern 1996 and 1997 calibrations of the Equator-S instrument.

Equator-S	HS side	LS side
Bern '96	2.20E-03	2.24E-05
Bern' 97	2.20E-03	3.01E-05

Table 4: Two calibration sets for the geometric factors on the Equator-S instrument.

Ideally, the g.f. should not change between the two Equator-S calibration sets and this holds true for the HS side. But on the LS side, it can be seen that the '97 calibration has a higher g.f. The LS g.f. for both calibration sets only use one file, both of which are the N2+ ion on pixel 11. There don't appear to be any problems on the '96 calibration file but in the '97 file it appears that the beam intensity changes during the run. Each step on each file contains a value for the beam monitor. Though this value cannot be used to measure the actual beam intensity (the beam monitor device is not directly in the path of the beam during file accumulation) the beam monitor value will show if there are any **changes** in the beam intensity. Making a plot of beam_mon verses time, it can be seen if the beam intensity changes throughout the file. Figure 18 below is representative of all files where the beam monitor does not vary more than 10% which is essentially constant. The one exception is shown on figure 19 where the beam intensity is clearly decreasing in the N2+, pixel 11 file from the '97 Bern calibration. Since beam intensity is an important factor in calculating the g.f., the '96 LS value is the most reliable.

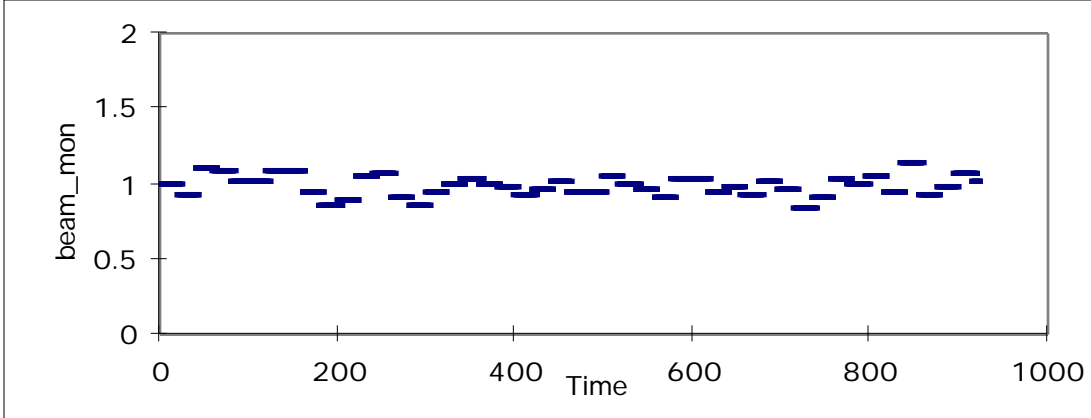


Figure 18: He+, pixel 2 from '96 Bern Equator-S calibration. Representative of all files.

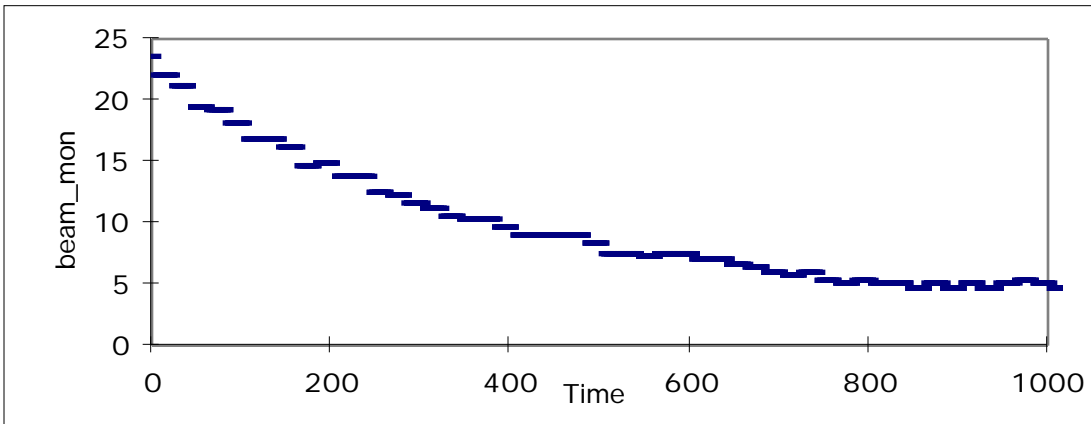


Figure 19: N2+, pixel 11 from the '97 Bern Equator-S calibration. Clearly the beam intensity is not constant.

The consistency in geometric factors between the Cluster models and between Cluster and Equator-S hold for the individual ions between all calibration models. Table 5 shows the average g.f. of the ions throughout all the CODIF calibration sets.

Ion	Average HS g.f.	Stand.Dev. HS g.f.
H+	2.9E-03	1.1E-03
He+	2.3E-03	0.4E-03
N+	2.0E-03	0.4E-03
N2+	1.6E-03	0.6E-03
O+	2.4E-03	N/A (single value)

Table 5: The HS geometric factors of each ion in the Cluster and Equator-S calibrations.

Note the standard deviation of all the ions is relatively low except the protons. The protons g.f. range went from 1.6E-03 to 5.1E-03.

PAC HV Conversion.

The supplies are calibrated for set voltage vs output. The conversion from digital setting to actual set voltage is given in the following table:

Set Val, mV	Set Val, Dec	Set Val, Hex	PacValue (V)
0	0.0	0	898
90	9.2	9	1000
181	18.6	12	2000
452	46.4	2E	5000
679	69.6	45	7500
905	92.8	5C	10000
1134	116.3	74	12500

The conversion is linear and assumes a slope of 9.75 mv/decimal setting.

From the table above, the PAC conversion for the Equator-S instrument is given by:

$$\text{PAC output (kV)} = (0.107494) * \text{pacset (dec)} + 0.010464$$

where pacset(dec) is the decimal PAC setting. The following table gives the voltages for some key settings.

PAC set Hex	PAC set Dec	Fitted PAC out
0	0	0.010
10	16	1.730
20	32	3.450
30	48	5.170
40	64	6.890
50	80	8.610
60	96	10.330
70	112	12.050
80	128	13.770
8d	141	15.167
90	144	15.490
A0	160	17.210
B0	176	18.929
C0	192	20.649
D0	208	22.369
E0	224	24.089
F0	240	25.809
FF	255	27.422